Hindawi Publishing Corporation
Journal of Robotics
Volume 2010, Article ID 139634, 11 pages
doi:10.1155/2010/139634

Research Article

Motion Intention Analysis-Based Coordinated Control for Amputee-Prosthesis Interaction

Fei Wang,[1,2] Shiguang Wen,[1] Chengdong Wu,[1] Yuzhong Zhang,[1] and Jincheng Li[1]

[1] *The institute of Artificial Intelligence & Robotics, College of Information Science & Engineering, Northeastern University, 110004 Shenyang, China*
[2] *State Key Laboratory of Robotics & Systems, Harbin Institute of Technology, 150001 Harbin, China*

Correspondence should be addressed to Fei Wang, wangfei@ise.neu.edu.cn

Received 1 November 2009; Revised 25 February 2010; Accepted 24 March 2010

Academic Editor: Zeng-Guang Hou

To study amputee-prosthesis (AP) interaction, a novel reconfigurable biped robot was designed and fabricated. In homogeneous configuration, two identical artificial legs (ALs) were used to simulate the symmetrical lower limbs of a healthy person. Linear inverted pendulum model combining with ZMP stability criterion was used to generate the gait trajectories of ALs. To acquire interjoint coordination for healthy gait, rate gyroscopes were mounted on CoGs of thigh and shank of both legs. By employing principal component analysis, the measured angular velocities were processed and the motion synergy was obtained in the final. Then, one of two ALs was replaced by a bionic leg (BL), and the biped robot was changed into heterogeneous configuration to simulate the AP coupling system. To realize symmetrical stable walking, master/slave coordinated control strategy is proposed. According to information acquired by gyroscopes, BL recognized the motion intention of AL and reconstructed its kinematic variables based on interjoint coordination. By employing iterative learning control, gait tracking of BL to AL was archived. Real environment robot walking experiments validated the correctness and effectiveness of the proposed scheme.

1. Introduction

Lower limb prosthesis is used to compensate the locomotion function for amputees in the field of biomedical rehabilitation. Conventional mechanical prosthesis has been criticized for difficulty in motion transformation, stiff-legged gait and poor mobility under complex condition. Intelligent prosthetic leg controlled by a microprocessing unit can realize the arbitrary gait precisely to coordinate with the sound leg of amputee [1]. It has been a challenging endeavor for interaction between amputee and prosthesis for their different structures, actuation manners, cognitive competence, and dynamic characters. To realize coordinated movement, prosthetic leg must be able to perceive the motion intention of amputee properly so as to actuate its joints accordingly when walking on different terrains with various cadences and stride length.

To guarantee the performance of prosthetic leg during development stage, a great amount of repetitive experiments that need amputee to participate entirely is necessary. It is not only costly but also painful to handicapped person, and even leads to accidental injury to amputee. Moreover, individual difference also makes it difficult to obtain the uniform and quantitative performance evaluation for prosthetic leg.

To solve problems mentioned above, a novel reconfigurable test-bed for prosthetic leg development is designed and fabricated by the Robotics Group at Northeastern University, China [2], which has two kinds of form called homogeneous configuration and heterogeneous configuration separately. The former is mainly used to study the symmetrical locomotion as many common biped robot systems [3, 4]. The latter, however, provides an ideal platform for the study of multiagent coordination, gait tracking and interaction for AP coupling system.

In this research, the heterogeneous configuration of test-bed is used to validate the master/slave dual-leg coordination strategy of the AP coupling system, motion intention recognition, and gait tracking based on iterative learning control.

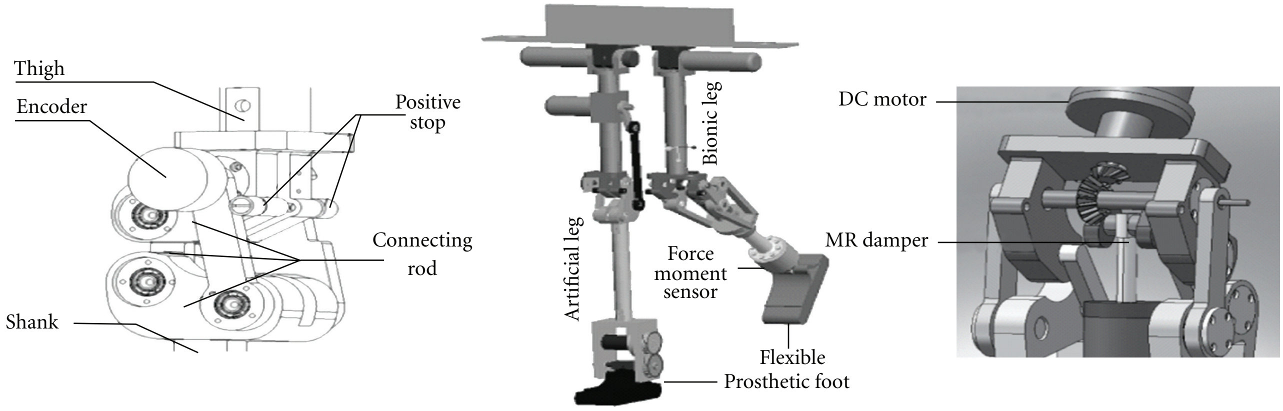

Figure 1: The test-bed in heterogeneous configuration and 4-bar knee joint mechanism.

In this architecture, the master is the sound leg of amputee, corresponds to AL in the test-bed. It generates the active motion that is planned by linear inverted pendulum model combining with ZMP stability criterion. The desired joint angle trajectory is then calculated by inverse kinematics of AL. The slave, however, is prosthetic leg, corresponds to the BL in the test-bed. It perceives the motion intention of the master, and controls itself making gait tracking to realize the coordination to the master.

2. Heterogeneous Biped Robot

Figure 1 shows the prototype of the test-bed in heterogeneous configuration that is mainly made up of two legs, one is AL used to simulate the sound leg of amputee and another is BL used to simulate stump with prosthetic leg. The two agents are heterogeneous at the aspect of mechanism, actuation manner, sensing capacity, and dynamic characteristics.

To realize humanoid gait, both legs are designed and fabricated with 4-bar closed-chain knee joints and flexible prosthetic foot. Joints in AL are actuated by Maxon DC servo-motors, which can realize arbitrary gait. The knee joint of BL are driven by a hybrid actuation system combing magneto-rheological (MR) damper augmented with a DC motor. Hybrid actuation manner greatly improves the mobility and environmental adaptability at the cost of a small rise in energy consumption.

3. Dual-Leg Coordination

3.1. Overview of Dual-Leg Coordinated Control. Dual-arm and multileg coordination are hot topics in the field of multirobot system research [5–7]. Dual-leg coordination belongs to the stable walking control of biped robot. In the past studies, however, the two legs were usually thought as a bifurcate mechanism of a single biped robot, the gait for the two legs are planned concurrently. Status information and command for both legs can be exchanged directly without the need of perception and the two legs are controlled as a whole by one locomotion controller. The concepts and methods of dual-leg coordination were not explicitly proposed for single biped robot control before.

Though quite similar to the dual-arm coordination at the aspect of system task, control principle and implementation method, dual-leg coordination is more difficult due to its complicated constrains. Table 1 shows the comparison for the two kinds of coordination.

According to control strategy, coordination methods of dual-arm and multileg can be roughly divided into two categories, named master/slave method and object-oriented method separately [8]. The former studies the motion tracking of slave arm (leg) to master arm (leg) by satisfying the constrain conditions of kinematics and dynamics; while the latter studies the tracking of desired motion trajectory and/or force trajectory for task object without considering the details of two arms (legs). For the simplicity of the master/slave method, the coordination capacity and adaptability is limited by the master/slave relations. Object-oriented method accords with the essence of human dual-arm (leg) coordination, however, control algorithm is comparatively complicated. The prosthetic leg has limitations at the aspect of intelligence and maneuverability. Therefore, master/slave strategy is suitable to AP coupling system.

According to task, dual-arm coordination can be divided into convey coordination and assemblage coordination. For biped robot, the system task can be described as: the two legs support the HAT, simultaneously, moving it smoothly through coordination to achieve stable walking of the whole biped locomotive system. Therefore, dual-leg coordination can be thought as a special form of convey coordination. Although the differences in terms of mechanism and actuation manner for the two legs, master/slave coordination method can be used in heterogeneous biped robot for the same basic configurations (e.g., length of leg, motion range of joints, etc.) and similar gait pattern for both legs. In dual-leg coordination system, AL is defined as master leg and BL as slave one. A coordination module is usually constructed and used to control the pose and position of interfaces between the HAT and the two legs to satisfy the constrain conditions of kinematics and dynamics. Therefore, motion planning, control, and compensation of the coordination module become key problems in coordinated control system research for AP coupling system.

3.2. Coordinated Control Architecture. For the complicated control task, the distributed hierarchical control architecture is used to realize the master/slave coordination for AP coupling system. Hierarchical architecture [9] is an advanced control structure in which the complicated task is decomposed into several levels according to the intelligent grade. For different levels, a certain control strategy and implementation method is used and the complicated task can be accomplished by all levels through interrelation and coordination. By using hierarchical control architecture, fault debugging and system implementation can be easily achieved.

According to master/slave relation, two independent hierarchical control systems were built for both legs as shown in Figure 2. Either consists of three levels, named task layer, plan layer and drive layer separately.

In the hierarchical control architecture of AL, the task layer has the highest intelligent grade and decides what to do according to environment information or human command. As a master leg, AL decides the task of the whole system, which usually includes level-walking at different speed, walking on stairs and slopes, running, emergency acts, and so forth. Plan layer has the middle intelligent grade and is used to plan the gait to realize the desired task. In plan layer, the kinematics and dynamics equations are solved for gait control purpose, also the planned gait is verified whether satisfying constrain conditions of the coordination model. Drive layer has the lowest intelligent grade, in which DC motors actuate joints to produce planned gait based on Fuzzy-PID feed-back control algorithm.

As a slave leg, the task of BL is to track the gait of AL to realize gait synergy. The task layer of BL is used to realize the functions of gait measurement, gait recognition, and gait estimation. In plan layer, a major work is to calculate the desired damper force and motor torque to realize gait tracking. In drive layer, a MR damper augmented by DC motor actuates the knee joint of BL according to the optimized damper force and motor torque obtained in plan layer, and a PD feed-back control algorithm is applied on the MR damper and Fuzzy-PID feed-back control algorithm is applied on the DC motor.

4. Gait Planning for Artificial Leg

4.1. Modeling. Figure 3 shows the mass and geometry models of test-bed in homogeneous configuration.

It is modeled as a system of 11 material points. Each link has its weight at the position of its CoG. The trunk is counted as the base link. In this research, however, it is assumed that the robot is held in 2D space. The movement of the robot is considered only in sagittal plane. Therefore, it has 6 DOF for gait planning.

4.1.1. Kinematics. First, direct kinematics of AL in swing phase is established in the coordinate system $\sum XYZ$ and the matrix of transformation from torso to ankle is expressed in (1).

4-bar mechanism in knee joint of AL brought the closed-chain geometrical constrain with kinematics that is expressed in (2), which makes two of the angle variables in $\theta_2^a, \theta_3^a, \theta_4^a,$ and θ_5^a dependent.

$$A^a = \begin{bmatrix} x_a^a \\ 0 \\ z_a^a \end{bmatrix} = \begin{bmatrix} -l_3^a \sin\theta_3^a - l_2^a \sin\theta_2^a - l_5^a \sin\theta_5^a - l_{11}^a \sin(\alpha - \theta_2^a) - l_{12}^a \sin(\beta - \theta_5^a) + x_h^a \\ 0 \\ -l_3^a \cos\theta_3^a - l_2^a \cos\theta_2^a - l_5^a \cos\theta_5^a + l_{11}^a \cos(\alpha - \theta_2^a) + l_{12}^a \cos(\beta - \theta_5^a) + z_h^a \end{bmatrix}, \tag{1}$$

$$\begin{aligned} f_1 &: (l_{11}^a - l_9^a)\cos(\theta_2^a - \alpha) + l_{10}^a \cos(\theta_5^a - \beta) \\ &\quad - l_3^a \cos\theta_3^a + l_4^a \cos\theta_4^a = 0, \\ f_2 &: (l_{11}^a - l_9^a)\sin(\theta_2^a - \alpha) + l_{10}^a \sin(\theta_5^a - \beta) \\ &\quad - l_3^a \sin\theta_3^a + l_4^a \sin\theta_4^a = 0. \end{aligned} \tag{2}$$

4.1.2. Dynamics. In swing phase, hip joint makes translational movement along a certain trajectory; in the meanwhile thigh and shank make rotational movement. If the generalized coordinate $\theta = [x_{1c}\ \ z_{1c}\ \ \theta_2^a\ \ \theta_3^a\ \ \theta_4^a\ \ \theta_5^a\ \ \theta_6^a]^T$ that θ_4^a and θ_5^a are the dependent variables, then the Lagrange function can be formed as

$$L_{sw}^a = \sum_{i=2}^{6}\left[\frac{1}{2}m_i^a(\dot{x}_{ic}^2 + \dot{z}_{ic}^2) + \frac{1}{2}J_i\dot{\theta}_i^{a^2} - m_i^a g z_{ic}\right]. \tag{3}$$

The drive forces of robot dynamic system are F_1^x, $F_1^z, T_2^a,\ T_3^a,\ T_4^a,\ T_5^a,$ and T_6^a. According to principle of virtual work, the virtual work of drive force is calculated by

$$\begin{aligned} \delta A = {} & F_1^x \delta x_{1c} + F_1^z \delta z_{1c} + (T_2^a - T_3^a - T_4^a)\theta_2^a + (T_3^a - T_5^a)\theta_3^a \\ & + (T_4^a - T_5^a)\theta_4^a + (T_5^a - T_6^a)\theta_5^a + T_6^a\theta_6^a. \end{aligned} \tag{4}$$

Then the generalized force is

$$\begin{aligned} Q = [&F_1^x \quad F_1^z \quad T_2^a - T_3^a - T_4^a \quad T_3^a \\ &- T_5^a \quad T_4^a - T_5^a \quad T_5^a - T_6^a \quad T_6^a], \end{aligned} \tag{5}$$

where F_1^x and F_1^z are the forces supplied by the HAT; T_4^a and T_5^a are the redundancy drive force and are set to 0. Then the Lagrange equation of the first kind is deduced as

$$M_{sw}^a(\theta^a)\ddot{\theta}^a + C_{sw}^a(\theta^a)\dot{\theta}^{a^2} + G_{sw}^a(\theta^a) = B_{sw}^a T^a + \lambda \dot{f}, \tag{6}$$

Table 1: Comparison between dual-arm and dual-leg coordination.

Items	Dual-arm coordination	Dual-leg coordination
System task	Grasping and holding object to track the target trajectory	Supporting and moving the HAT of biped robot to realize stable walking
Methods	Planning, control, and compensation of coordinated motion	
Controlled object	Homogeneous arms	Heterogeneous legs
Target object	Grasped and held object	The HAT (Head, Arms, and Torso)
Base	Fixed	Mobile
Control complexity	Relative simple	Complicated
Interface	Multiple fingers	Hip joints
Target trajectory	Task trajectory of grasped and held object	Gait trajectory for the center of HAT or the center of crotch
Mechanism	Closed chain all the time	Closed chain in stance phase Open chain in swing phase
Constrains	Kinematics and dynamics	Dynamic constrains for open chain and both for closed chain
Motion pattern	Different for two arms	Similar for two legs (phase-difference)

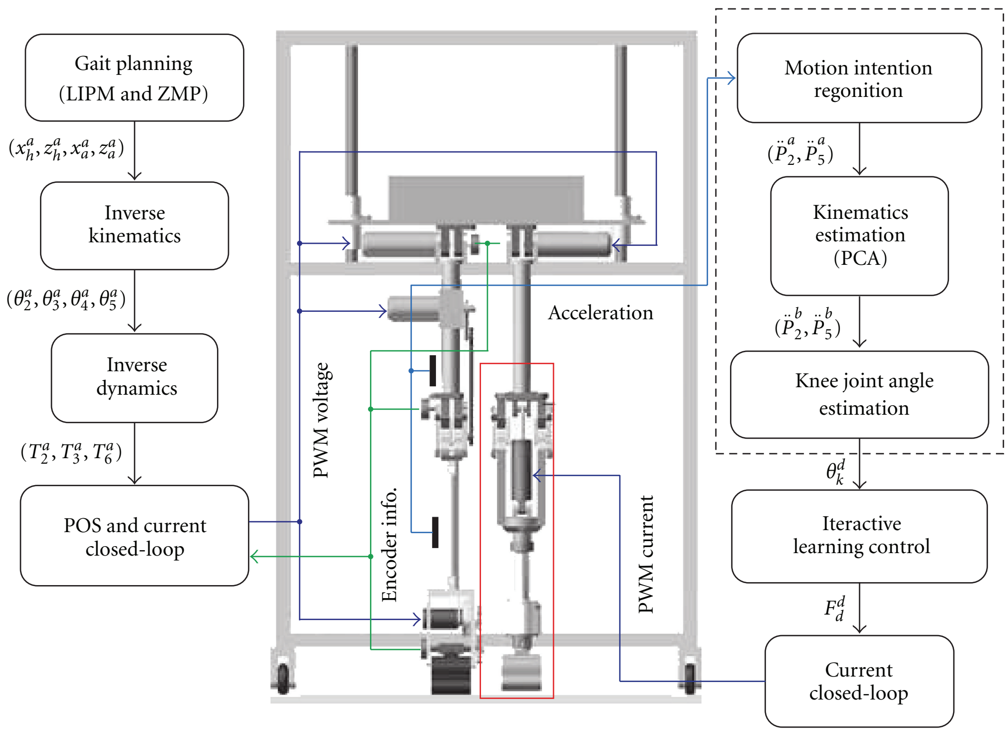

Figure 2: Coordinated control architecture.

where M_{sw}^a is a symmetric matrix called inertial matrix, C_{sw}^a is an antisymmetric matrix named centrifugal force or Coriolis force matrix, G_{sw}^a is matrix of gravitational forces, B is coefficient matrix of applied torques, and $\lambda \dot{f}$ represents constrain torque.

4.2. Gait Planning

4.2.1. ZMP Theory. One of the criterions for estimating the stability of the walking is a ZMP (Zero Moment Point) criterion proposed by Vukobratovic [10]. ZMP is a point on

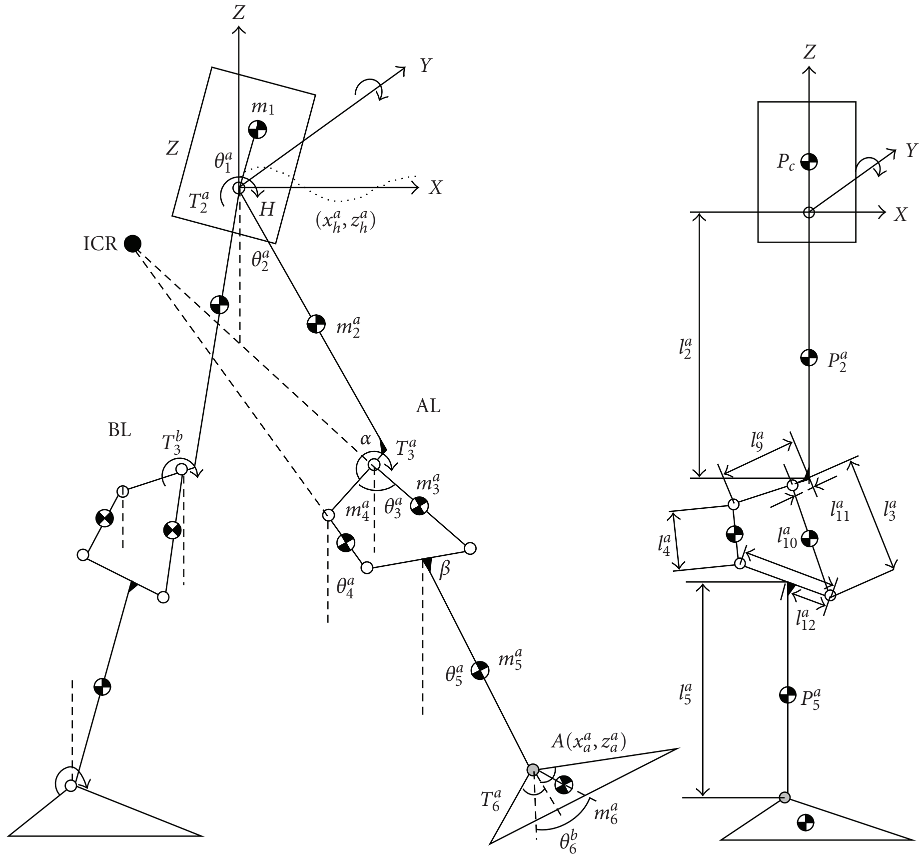

Figure 3: Mass and geometry models.

the surface about which the sum of all moments of active forces, momentums are equal to zero. The calculation of ZMP is described as follows

$$x_{\text{zmp}} = \frac{\sum_{i=1}^{n} m_i(\ddot{z}_i + g)x_i - \sum_{i=1}^{n} m_i\ddot{x}_i z_i + \sum_{i=1}^{n} M_{iy}}{\sum_{i=1}^{n} m_i(\ddot{z}_i + g)},$$
$$y_{\text{zmp}} = \frac{\sum_{i=1}^{n} m_i(\ddot{z}_i + g)y_i - \sum_{i=1}^{n} m_i\ddot{y}_i z_i + \sum_{i=1}^{n} M_{ix}}{\sum_{i=1}^{n} m_i(\ddot{z}_i + g)}, \tag{7}$$

where m_i is the mass, (x_i, y_i, z_i) is the Cartesian coordinate of CoG of i^{th} link, $(x_{\text{zmp}}, y_{\text{zmp}})$ is the Cartesian coordinate of ZMP.

While a biped robot is standing still or walking very slowly, a projective point of the CoG on the surface is in the polygon made from the contact points on the sole. In the case, the robot is in the statically stable state and keeps on walking without a tumble. However, while the body and/or the legs are moving fast, various accelerations due to motions are produced, and the projective point of the center of gravity is getting out of the polygon. ZMP is like a projective point of the CoG in the standing still state or the slow-walking state of the robot while the robot is in the dynamic-walking state. According to the ZMP criterion, the robot may keep walking without tumbling. In this study, based on the ZMP criterion, the gait planning for AL in the sagittal plane is designed.

4.2.2. Linear Inverted Pendulum Model. Bipedal walking system is complex, nonlinear, and naturally unstable. Linear inverted pendulum model (LIMP) theory provides an alternative approach to generate the gait trajectory of bipedal walking. Figure 4 shows the LIMP model and CoG transform model in a sagittal plane.

Where f is the stretching force imposed on the stick. τ is the moment generated by ground reaction force, θ is the angle of stick inclination (the clockwise direction is positive), M is the concentrated mass representing the HAT, and r is the length of the stick. The mass of the stick is neglected.

By using Lagrangian function approach, the dynamics model of LIPM can be deduced by

$$\frac{d}{dt}\left(\frac{\partial L}{\partial \dot{q}}\right) - \frac{\partial L}{\partial q} = Q,$$
$$L = T - V = \frac{1}{2}mr^2\dot{\theta}^2 + \frac{1}{2}m\dot{r}^2 - mgr\cos\theta, \tag{8}$$
$$q = [\theta r]^T, \quad Q = [f\tau]^T,$$

where L is Lagrangian function, q is generalized coordinate and Q is the generalized force. Then the dynamics function of LIMP is expressed as

$$mr^2\ddot{\theta}^2 + 2mr\dot{r}\dot{\theta} + mgr\sin\theta = \tau,$$
$$m\ddot{r} - mr\dot{\theta}^2 + mg\cos = f. \tag{9}$$

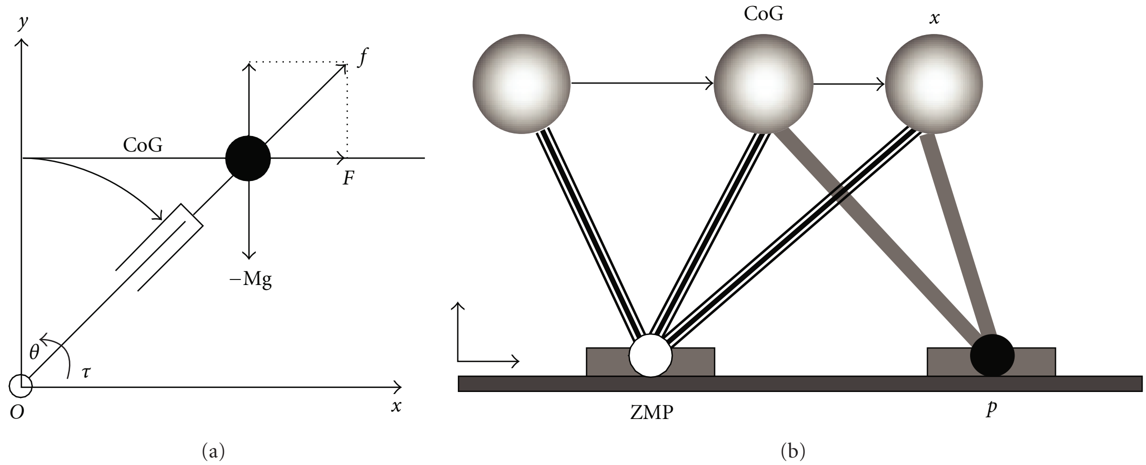

Figure 4: LIMP model and CoG transform model in sagittal plane.

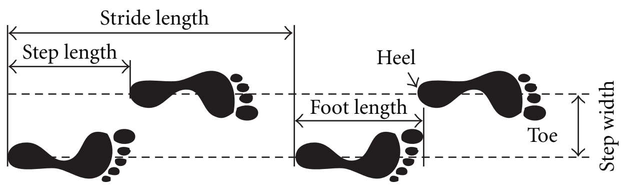

Figure 5: Gait spatial features.

In order to keep the movement of the CoG in the horizontal direction and get an acceleration motion, the stretching force f and mass m must satisfy the relation as

$$\begin{aligned} f\cos\theta &= mg, \\ f\sin\theta &= m\ddot{x}. \end{aligned} \tag{10}$$

Solving this equation can get

$$x - p = \frac{g}{z}\ddot{x}, \tag{11}$$

where x is the length of the projection of the CoG in x-axis, and z is the height of CoG in z-axis, p is the projection of ZMP in x-axis.

4.2.3. Gait Planning for AL. The gait space features of human walking are shown in Figure 5. By set time-spatial features of AL as shown in Table 2, the corresponding ZMP trajectory can be obtained as shown in Figure 6.

In LIMP, the relation between ZMP and CoG is expressed

$$\begin{aligned} \ddot{x} &= \frac{g}{z}\left(x - x_{\text{zmp}}\right), \\ \ddot{y} &= \frac{g}{z}\left(y - y_{\text{zmp}}\right). \end{aligned} \tag{12}$$

The trajectories of ZMP was planned as mentioned above, then the trajectories of CoG can be calculated by (12), the ideal trajectories of ZMP and CoG in X and Y axial directions are shown in Figure 7.

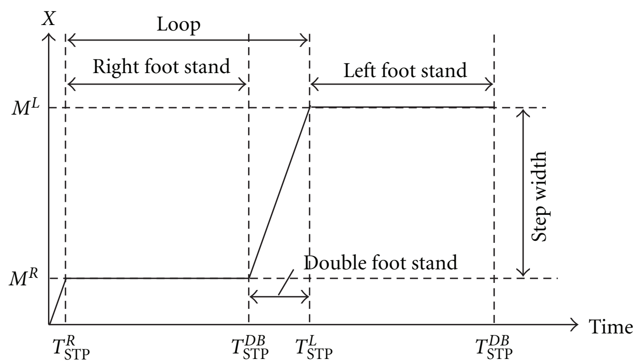

Figure 6: Ideal ZMP trajectories.

Table 2: Gait parameters of AL.

Item	Value
Thigh length	0.46 m
Shank length	0.48 m
Foot height	0.10 m
Foot width	0.07 m
Foot length	0.25 m
Horizontal distance between ankle joint and heel	0.055 m
Gait velocity	95∼125 step/min
Step length	0.20∼0.50 m
Step width	0.10 m
Step height	0.05∼0.10 m
Stride length	0.75∼0.83 m
Gait cycle	1.20 s

Gait in Cartesian space is intuitive, easy to describe, and good to reflect the relation between robot system and ground. However, the movement of artificial leg is achieved by the rotation of joints. Therefore, the solving of inverse kinematics is needed to map the variables from

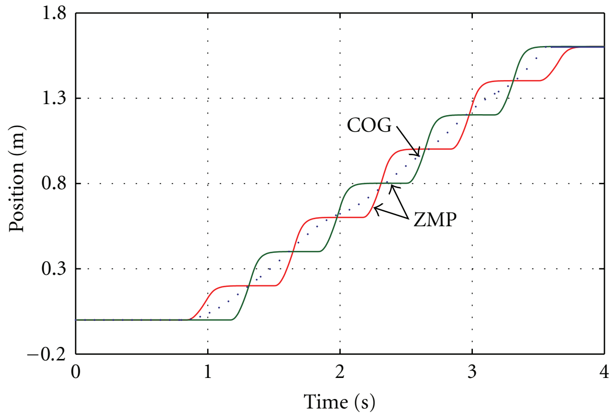

(a)

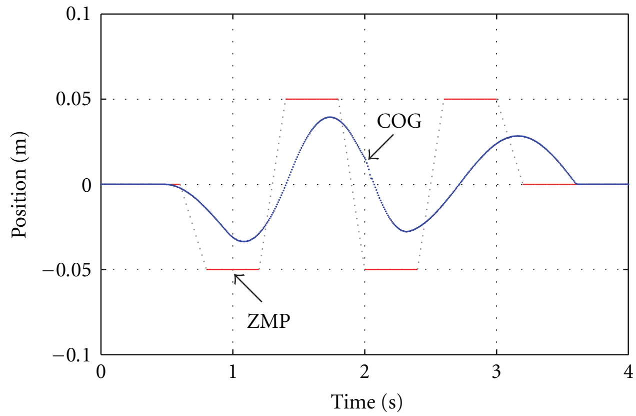

(b)

Figure 7: ZMP and CoG trajectories in X and Y axial directions.

Cartesian space to joint space. In this research, the Newton-Raphson algorithm is used to calculate the joint angles of AL. Figure 8 shows the desired angles of hip joints of both leg, angles of knee and ankle joints of AL separately, which are calculated through inverse kinematics. In general, above-knee amputee always has an intact hip, so that there is only an angular phase difference between hips of sound leg and stump. The ankle of BL is fixed without the need to gait plan. The angle of knee joint in BL should be estimated based on interjoint coordination described in the following section.

5. Gait Recognition and Estimation for Bionic Leg

Although amputee and his/her artificial limb (prosthesis) can exchange information directly through electromyography (EMG) or biological neural signal, EMG and neural signal-based prosthesis techniques are still premature. For common prosthesis, movement intention of amputee can only be perceived by its own perception system. In this research, embedded 3-axial attitude sensor can measure kinematic information of the thigh that reflects the amputee's posture and walking conditions. Based on these measured data, gait pattern of BL can be estimated by tuned gait classifier so that MR damper can drive the knee joint to coordinate with the sound leg of amputee to realize symmetrical stable walking.

In recent years, inertial motion capture has emerged as one of the most versatile methods of full-body ambulation measurement. By using sensor fusion of three-axis gyroscopes and three-axis accelerometers, inertial sensors accurately measure the orientation and position of body segments in a global coordinate system in this research. The nature of the sensor technology used allows inertial motion capture systems to overcome some of the most pressing limitations found in alternative methods such as optical, mechanical, acoustic, and magnetic motion capture.

5.1. Overview of Principal Component Analysis. Principal component analysis (PCA) is a general approach to compression and dimensionality reduction for mass data based on multivariable statistical analysis. The basic idea of PCA is to attempt to efficiently represent the data by decomposing a data space into a linear combination of a small collection of bases consisting of orthogonals that maximally preserves the variance in the data. If n measurements of m-tuple $X^T = (x_1, x_2, \ldots, x_m)$ represent original data with linear correlations, then the jth principal component (PC) can be expressed as

$$P_j = a_{j1}x_1 + a_{j1}x_2 + \cdots + a_{jm}x_m \sum_i a_{ji}^2 = 1. \qquad (13)$$

The coefficients $a_{ji}(i = 1, 2, \ldots, m)$ are called the factor loadings. The magnitude indicates the amount of variation in variable x_i that is captured by the principal component P_j and the sign indicates the nature of correlation between P_j and x_i. For a given data set, PCA produces a unique solution. The common procedure of PCA can be summarized as the following 4 steps.

(1) *Normalization of Original Data.* In order to perform PCA, the data need to have zero mean as well as stand deviation of 1 and the normalization can be achieved by

$$\begin{aligned} x_{ij}^* &= \frac{x_{ij} - \mu_i}{\sigma_i}, \\ \mu_i &= \frac{\sum_{j=1}^n x_{ij}}{n}, \\ \sigma_i &= \sqrt{\frac{\sum_{j=1}^n \left(x_{ij} - \mu_j\right)}{(n-1)}}, \end{aligned} \qquad (14)$$

where $i = 1, 2, \ldots, m$; $j = 1, 2, \ldots, n$.

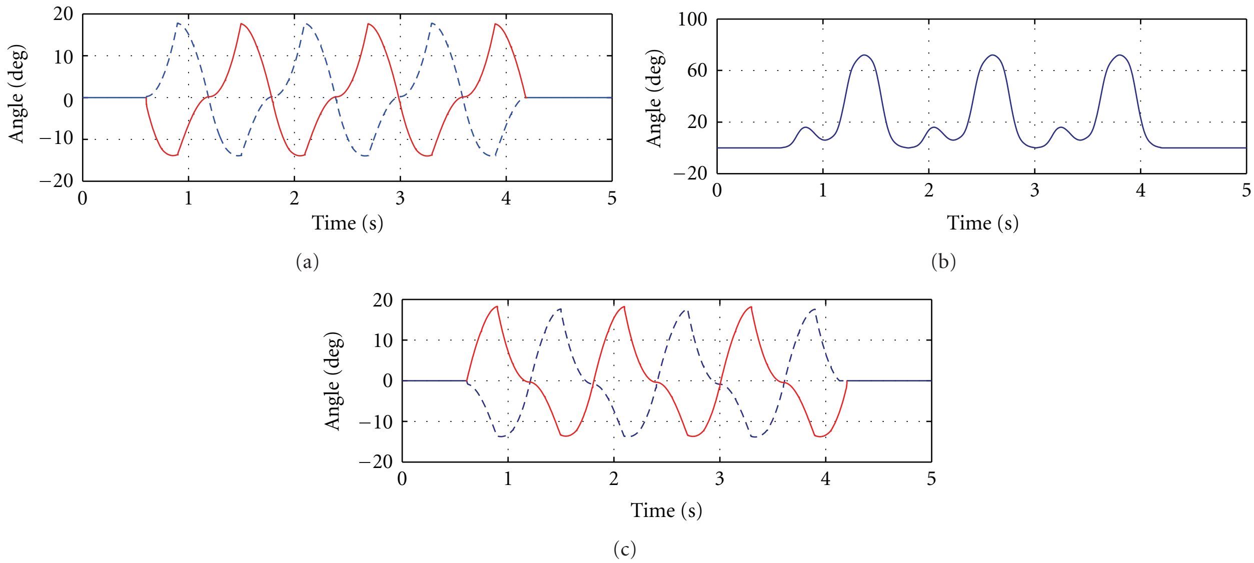

Figure 8: Desired angles of hip joint, knee joint, and ankle joint.

(2) *Calculation of Covariance Matrix R.* We have

$$R = \frac{1}{N-1} X^{*T} X^{*}, \tag{15}$$

where X^* is the normalized matrix of X.

(3) *Determination of the Number of PC.* The eigenvectors are obtained algebraically through decomposition of the covariance matrix R of the original data. If the eigenvalue λ_i $(i = 1, 2, \ldots, m)$ and eigenvector γ_i $(i = 1, 2, \ldots, m)$ are given, the number of PC p can be determined by

$$\eta_i = \frac{\lambda_i}{\sum_{i=1}^{m} \lambda_i}, \qquad \epsilon(p) = \sum_{i=1}^{p} \eta_i, \tag{16}$$

where p satisfies $\epsilon(p) \geq 85\% \sim 90\%$.

(4) Determination of Transformation matrix Γ. The transformation matrix Γ formed by the p eigenvectors of matrix R sorted in descending order of the corresponding eigenvalue

$$\Gamma = \left(\gamma_1, \gamma_2, \ldots \gamma_p\right) \tag{17}$$

which maps X on the new coordinates P with

$$P = \Gamma^T X. \tag{18}$$

5.2. Reconstruction of BL's Kinematics Using AL's Kinematics. In human gait, it has been observed that joint angle trajectories show strong linear correlations [11–13], which indicates that a compressed gait data set can be obtained by using PCA. If the original gait data X is acquired by sensors and preprocessed, the orthogonal unit eigenvector γ_i $(i = 1, 2, \ldots, m)$ and transformation matrix $R = (\gamma_1, \gamma_2, \ldots, \gamma_m)$ can be obtained and the new gait variables can be expressed as

$$Y = R^T X. \tag{19}$$

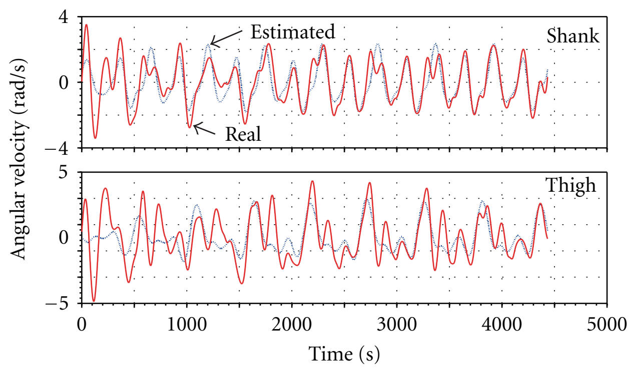

Figure 9: Motion estimation of IBL.

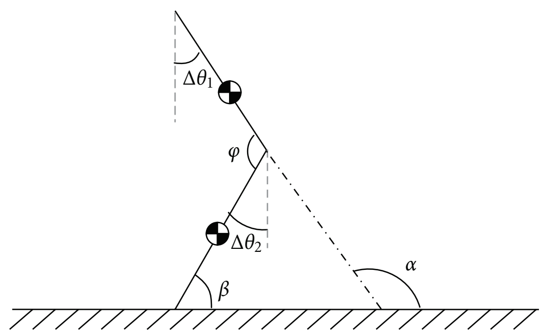

Figure 10: Lower limb joints geometry.

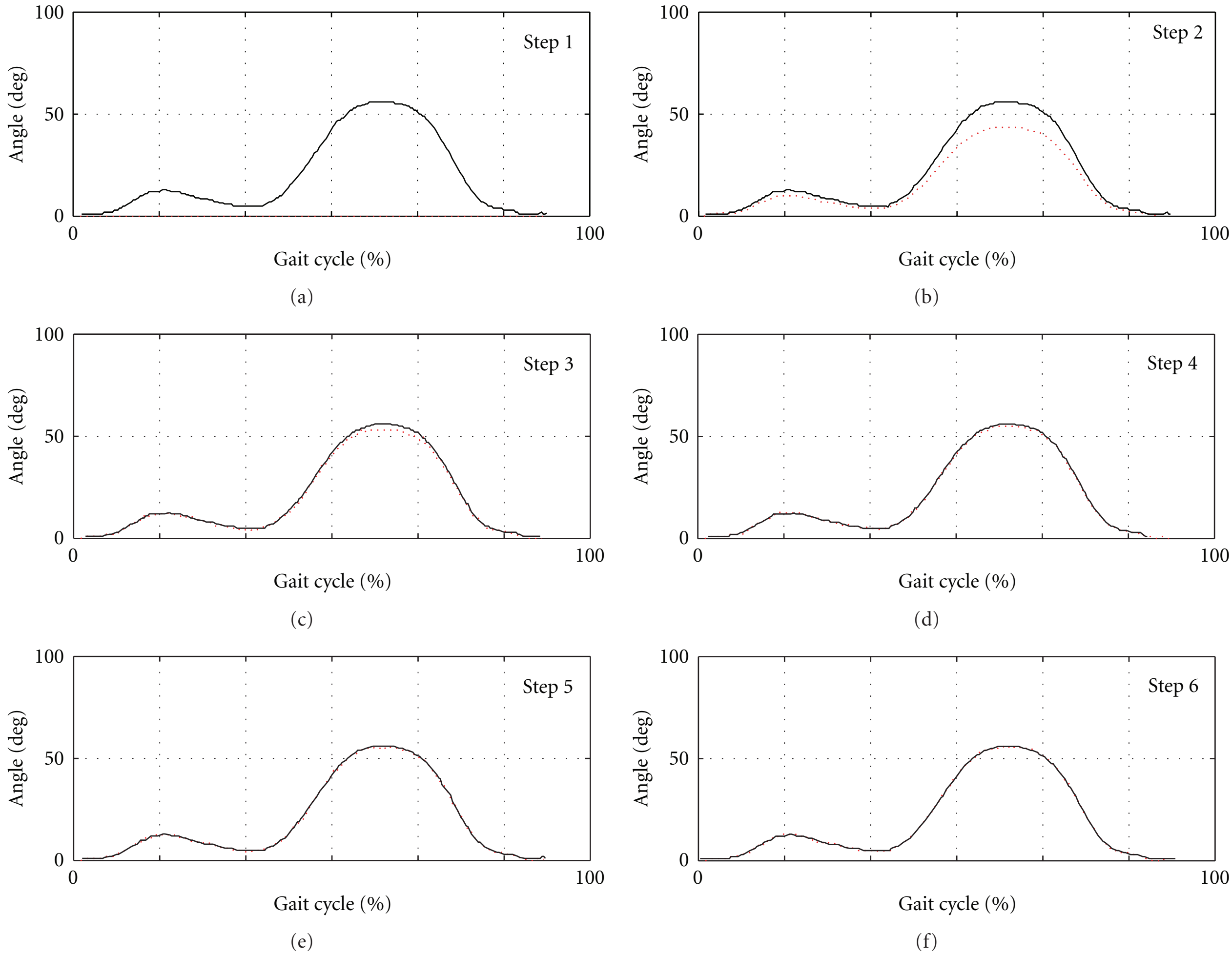

Figure 11: Tracking curve of IBL knee joint relative angle with P-type open/closed-loop ILC.

Since R is orthogonal matrix, X can be reconstructed from Y by

$$X = RY. \tag{20}$$

If p is determined, then the equation can be rewritten as

$$X = \Gamma Y^*, \tag{21}$$

where $\Gamma = (\gamma_1, \gamma_2, \ldots, \gamma_p)$, Y^* is the top p rows of Y. Neglecting the last components of Y, the data is reduced in a way that the least information is lost. A reconstruction of X from the lower dimensional coordinate Y^*, leads to a least-square optimal fit of the original data. PCA cannot only be used for compression, but also for reconstruction of incomplete measurements.

Assuming that the first components of $X_1 \in \mathbb{R}^{(m-l)}$ of X are known, and the remaining part $X_2 \in \mathbb{R}^{(l)}$ is unknown, (21) is separated into

$$X_1 = \Gamma_1 Y^*, \quad X_2 = \Gamma_2 Y^*, \tag{22}$$

where $\Gamma_1 \in \mathbb{R}^{(m-l)\times p}$ and $\Gamma_2 \in \mathbb{R}^{l\times p}$ are the sub matrix of Γ. Thus X_2 is reconstructed from X_1 by

$$X_2 = \Gamma_2 \left({\Gamma_1}^T \Gamma_1\right)^{-1} {\Gamma_1}^T X_1. \tag{23}$$

For AP coupling system, the observable data is the motion of sound leg, and the missing data is the motion of BL. To obtain the covariance matrix R, the test-bed was firstly configured as homogeneous form, CoGs of thigh and shank of two identical ALs were mounted with rate gyroscopes, and walking experiments were conducted with various cadences and stride length. The acquired data from gyroscopes were treated by following the procedures described above and the covariance matrix was obtained in the final. Then the test-bed is reconfigured as heterogeneous form and a pair of rate gyroscope mounted on the CoGs of thigh and shank was used to measure the motion of AL. By employing PCA, the motion of BL is estimated as shown in Figure 9. Solid line represents real angular velocities obtained by gyroscopes mounted on AL, while dashed line represents estimated angular velocities of BL calculated through (23).

By integrating angular velocities of thigh and shank calculated above, the angles $\Delta\theta_1$ and $\Delta\theta_2$ can be obtained.

Figure 12: Step sequence in swing phase.

Then the angle between the thigh and ground α and the angle between the shank and ground β can be calculated according to the geometric relation as shown in Figure 10

$$\alpha = 90 + \Delta\theta_1,$$
$$\beta = 90 - \Delta\theta_2. \tag{24}$$

Then the angle of knee joint of BL can be estimated by

$$\varphi = 180 - \alpha + \beta. \tag{25}$$

6. Gait Tracking for Bionic Leg

Gait tracking control is the key to realize stable walking of AP coupling system, which belongs to time-varying trajectory tracking problem. In the heterogeneous configuration of test-bed, MR damper and electro-motors are used to actuate the joints tracking the ideal trajectories predefined in gait planning strategy. Due to the complicated dynamical characters of nonlinear, time-varying, strong coupling, and the need of high precise repetitive motion, gait tracking control is a hard difficulty in AP coupling research especially for BL that is hybrid-controlled by MR damper augmented with electro-motor. Although the methods, such as nonlinear decoupling control, decomposition feedback control, adaptive control, computed torque control, and so forth, were widely studied and proved able to solve time-varying trajectory tracking problem effectively, complex algorithm, time-consuming computation, and the need of precise and accurate system model limit the use of these methods in gait tracking control of AP coupling system. Iterative learning control (ILC) [14] can meet the special control requirement of gait tracking.

ILC can be stated as follows.It is due to repetitive motion that initial state is the same with the end $\theta_0(0)$ using preceding control input and actual output error, to find a best control input which will track the reference trajectories in limited time, that is, $\theta_k(t) \rightarrow \theta^d(t)$; $u_k(t) \rightarrow u^d(t)$. $\theta^d(t)$ and $u^d(t)$ are the desired output and control input, and k is the number of iterative learning steps. In this paper, closed-loop ILC is combined with open loop ILC and the first order P-type open/closed-loop ILC is proposed. The control law is given by:

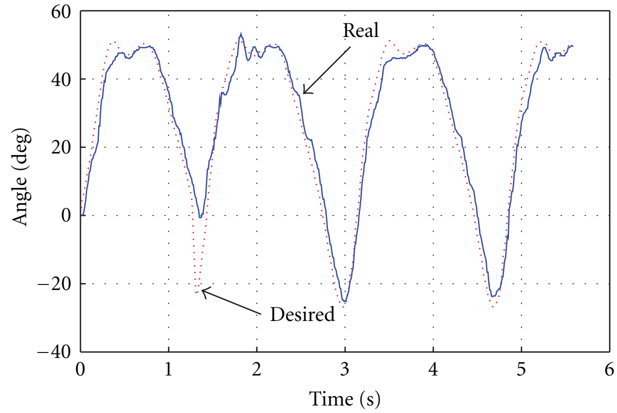

Figure 13: Real and desired hip joint angle of artificial leg during swing.

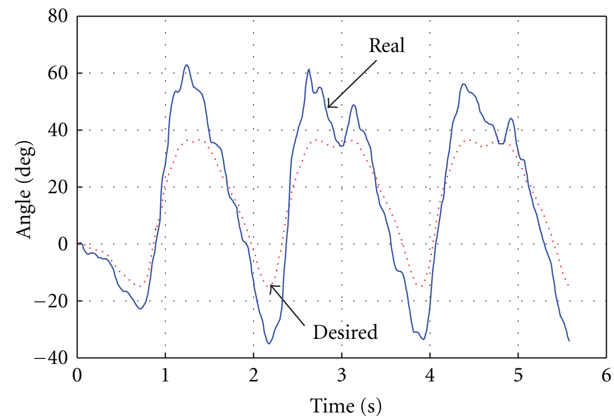

Figure 14: Real and desired hip joint angle of bionic leg during swing.

$$u_{k+1}(i) = u_k(i) + \Gamma e_{k+1}(i) + \Gamma' e_k(i), \quad k = 1, 2, \ldots, \tag{26}$$

where Γ and Γ' are the learning gains, $e_k(i) = \theta^d(t) - \theta(t)$ is the tracking error. Initial state, that is, $\theta_0(0) = \theta^k(0)$, must be satisfied in learning phase.

7. Experimental Results

To validate the effectiveness of the proposed coordinated control strategy for AP interaction, the virtual prototyping-based collaborative simulation and physical prototype experiments for stable walking control for biped robot were conduct.

Virtual prototype of test-bed is established using software ADAMS. Control module is built in MATLAB/Simulink. The sampling interval is 0.02 s and simulation time is 1.6 s. Relative knee joint angle tracking of BL to AL is illustrated

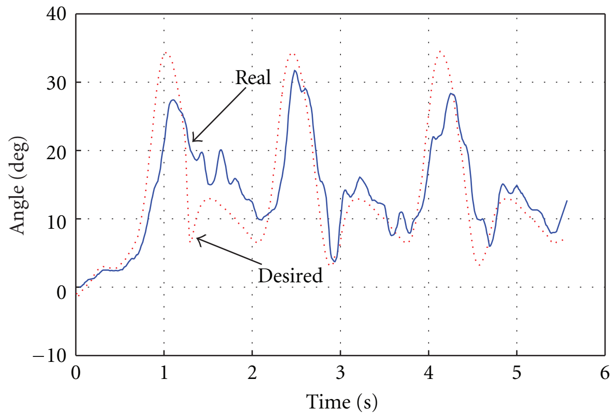

Figure 15: Real and desired knee joint angle of artificial leg during swing.

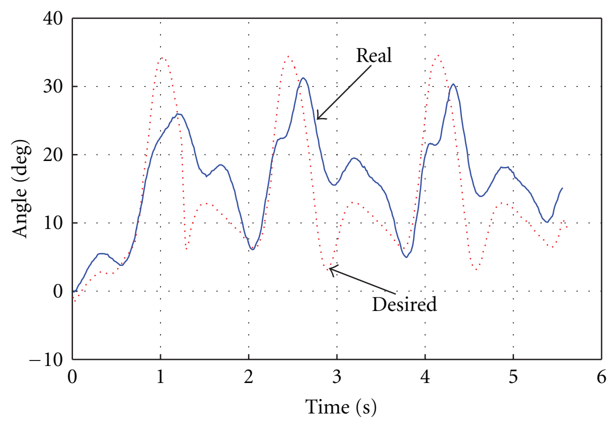

Figure 16: Real and desired knee joint angle of bionic leg during swing.

in Figure 11. The solid line represents reference knee joint angle estimated by method introduced in Section 5, while the dashed line represents the real output of ILC controller. From the figure, it can be seen that the learning was terminated after 6-step iterations when the error criterion was satisfied.

The simulation result indicates that BL controlled by hybrid actuation system can track the gait of AL well.

Figure 12 shows the gait tracking control in swing. Figures 13, 14, 15, and 16 shows the desired and real joint angles during experiment. The results shows that P-type open/close-loop ILC control scheme is effective and can insure the BL tracking gait of AL to realize stable walking of the whole system.

8. Conclusion

This paper describes the coordinated control for AP coupling system to realize symmetrical stable walking. The proposed scheme consists of walking gait synthesis, motion intention recognition, and gait tracking. Simulation and experimental results demonstrate that the proposed control scheme is correct and reasonable. The master/slave dual-leg coordinated control strategy is suitable for complex AP coupling system.

Acknowledgments

This work was supported by the Nature Science Foundation of China (Grant no. 60705031), by Specialized Research Fund for the Doctoral Program of Higher Education (Grant no. 20070145105), by State Key Laboratory of Robotics and System (HIT) (Grant no. SKLRS200711), and by Fundamental Research Funds for the Central Universities (Grant no. N090404007).

References

[1] H. Herr and A. Wilkenfeld, "User-adaptive control of a magneto-rheological prosthetic knee," *Industrial Robot*, vol. 30, no. 1, pp. 42–55, 2003.

[2] F. Wang, C. D. Wu, Y. Z. Zhang, and X. H. Xu, "Virtual prototyping based collaborative simulation of biped robot with heterogeneous legs," in *Proceedings of the 13th International Conference on Advanced Robotics*, pp. 874–879, 2007.

[3] H. Lim, A. Ishii, and A. Takanishi, "Basic emotional walking using a biped humanoid robot," in *Proceedings of the IEEE International Conference on Systems, Man and Cybernetics*, vol. 4, pp. 954–959, 1999.

[4] S. Collins, A. Ruina, R. Tedrake, and M. Wisse, "Efficient bipedal robots based on passive-dynamic walkers," *Science*, vol. 307, no. 5712, pp. 1082–1085, 2005.

[5] N. Xi and T.-J. Tarn, "Sensor-referenced multiple robot cooperation for material handling," *Industrial Robot*, vol. 25, no. 2, pp. 129–133, 1998.

[6] H. G. Cai, H. Liu, and J. W. Li, "A survey of multi-fingered robot hands: issues of coordination and autonomous grasp," *Robot*, vol. 22, no. 4, pp. 319–328, 2000.

[7] V. Lippiello, L. Villani, and B. Siciliano, "An open architecture for sensory feedback control of a dual-arm industrial robotic cell," *Industrial Robot*, vol. 34, no. 1, pp. 46–53, 2007.

[8] C. Guodong, C. Wenshan, Z. Peng, and C. Jing, "Hybrid position/force control for dual-arm symmetric coordination-model algorithm and realization," *Acta Automatica Sinica*, vol. 22, no. 4, pp. 418–427, 1996.

[9] L. Jun, Z. Xinglong, and Y. Jingping, "Hierarchical control of dual-arm robot parts mate," *Manufacturing Automation*, vol. 24, no. 6, pp. 22–25, 2002.

[10] M. Vukobratovic, B. Borovac, and V. Potkonjak, "ZMP: a review of some basic misunderstandings," *International Journal of Humanoid Robotics*, vol. 3, no. 2, pp. 153–175, 2006.

[11] K. Harada, S. Kajita, K. Kaneko, and H. Hirukawa, "ZMP analysis for ARM/Leg coordination," in *Proceedings of the IEEE International Conference on Intelligent Robots and Systems*, vol. 1, pp. 75–81, 2003.

[12] A. Alexandrov, A. Frolov, and J. Massion, "Axial synergies during human upper trunk bending," *Experimental Brain Research*, vol. 118, no. 2, pp. 210–220, 1998.

[13] N. St-Onge and A. G. Feldman, "Interjoint coordination in lower limbs during different movements in humans," *Experimental Brain Research*, vol. 148, no. 2, pp. 139–149, 2003.

[14] S. Arimoto, S. Kawamura, and F. Miyazaki, "Bettering operation of robotics by learning," *Journal of Robotic Systems*, vol. 1, no. 2, pp. 123–140, 1984.